

Heavy neutrino signals at large hadron colliders

F. del Aguila¹, J. A. Aguilar-Saavedra¹, R. Pittau²

¹ *Departamento de Física Teórica y del Cosmos and CAFPE,
Universidad de Granada, E-18071 Granada, Spain*

² *Dipartimento di Fisica Teorica, Università di Torino, and INFN
Sezione di Torino, Italy*

Abstract

We study the LHC discovery potential for heavy Majorana neutrino singlets in the process $pp \rightarrow W^+ \rightarrow \mu^+ N \rightarrow \mu^+ \mu^+ jj$, plus its charge conjugate. With a fast detector simulation we show that, in contrast with previous claims, backgrounds involving two same-sign muons are not negligible and, moreover, they cannot be eliminated with simple sequential kinematical cuts. Using a likelihood analysis it is shown that, for heavy neutrinos coupling only to the muon, LHC has 5σ sensitivity for heavy neutrino masses up to 175 GeV. This reduction in sensitivity, compared to previous parton-level estimates, is driven by the $\sim 10^2 - 10^3$ times larger background. Approximate limits are also provided for other lepton number-violating final states, as well as for Tevatron. As a by-product of our analysis, heavy neutrino production has been implemented within the ALPGEN framework.

1 Introduction

Large hadron colliders involve strong interacting particles as initial states, giving rise to huge hadronic cross sections. The large luminosities expected will also provide quite large electroweak signals, with for instance 1.6×10^{10} (4×10^7) W bosons at LHC (Tevatron) for a luminosity of 100 (2) fb^{-1} . Therefore, these colliders can be used for precise studies of the leptonic sector as well, and in particular they can produce new heavy neutrinos at an observable level, or improve present limits on their masses and mixings [1–4] (see Ref. [5] for a review). These new fermions transform trivially under the gauge symmetry group of the Standard Model (SM), and in the absence of other interactions they are produced and decay only through their mixing with the SM leptons. With new interactions, like for instance in left-right models [6], heavy neutrinos can be also produced by gauge couplings unsuppressed by small mixing angles, yielding larger cross sections and implying a much higher collider discovery reach [7, 8]. In this

scenario, however, the observation of the new interactions could be more important than the existence of new heavy neutrinos.

We will concentrate on the first possibility, neglecting other new production mechanisms, what is a conservative approach. In this case, for example, it has been claimed by looking at the lepton number violating (LNV) $\Delta L = 2$ process $pp^{(\pm)} \rightarrow \mu^\pm \mu^\pm jj$ that LHC will be sensitive to heavy Majorana neutrinos with masses m_N up to 400 GeV, whereas Tevatron is sensitive to masses up to 150 GeV [2,4]. However, as we shall show, taking into account the actual backgrounds these limits are far from being realistic. In particular, backgrounds involving b quarks, as for instance $t\bar{t}nj$ (with nj standing for n additional jets), are two orders of magnitude larger than previously estimated. Moreover, in the region $m_N < M_W$ the largest and irreducible background is $b\bar{b}nj$, by far dominant but overlooked in previous analyses [4]. In this work we make a detailed study, at the level of fast simulation, of the LHC sensitivity to Majorana neutrinos in the process $pp \rightarrow \mu^\pm \mu^\pm jj$, which is the cleanest final state, for both $m_N > M_W$ and $m_N < M_W$. The generation of heavy neutrino signals has been implemented in the ALPGEN [9] framework, including the process studied here as well as other final states. In the following, after making precise our assumptions and notation in section 2, we describe the implementation of heavy neutrino production in ALPGEN in section 3. We present our detailed results in section 4, where we will eventually find that heavy neutrinos can be discovered up to $m_N = 175$ GeV, and that for a given “reference” mass $m_N = 60$ GeV the mixing can be probed at the 10^{-2} level. These figures are much less optimistic than others previously obtained in the literature. Estimates for Tevatron are given in section 5, and our conclusions are drawn in section 6.

2 Heavy neutrino interactions

Our assumptions and notation are reviewed with more detail in Ref. [5] (see also Refs. [10,11]). The SM is only extended with heavy neutrino singlets N_j , which are assumed to have masses of the order of the electroweak scale, up to few hundreds of GeV. We concentrate on the lightest one, assuming for simplicity that the other extra neutrinos are heavy enough to neglect possible interference effects. The new heavy neutrino N (where we suppress the unnecessary subindex) can have Dirac character, what requires the addition of at least two singlets, or Majorana, in which case $(N_L)^c \equiv CN_L^T = N_R$ and lepton number is violated. In either case it is produced and decays through its mixing with the light leptons, which is described by the interaction

Lagrangian (in standard notation)

$$\begin{aligned}
\mathcal{L}_W &= -\frac{g}{\sqrt{2}} \left(\bar{\ell} \gamma^\mu V_{\ell N} P_L N W_\mu + \bar{N} \gamma^\mu V_{\ell N}^* P_L \ell W_\mu^\dagger \right), \\
\mathcal{L}_Z &= -\frac{g}{2c_W} \left(\bar{\nu}_\ell \gamma^\mu V_{\ell N} P_L N + \bar{N} \gamma^\mu V_{\ell N}^* P_L \nu_\ell \right) Z_\mu, \\
\mathcal{L}_H &= -\frac{g m_N}{2M_W} \left(\bar{\nu}_\ell V_{\ell N} P_R N + \bar{N} V_{\ell N}^* P_L \nu_\ell \right) H.
\end{aligned} \tag{1}$$

The SM Lagrangian remains unchanged in the limit of small mixing angles $V_{\ell N}$, $\ell = e, \mu, \tau$ (which is the actual case), up to very small corrections $O(V^2)$. Neutral couplings involving two heavy neutrinos are also of order V^2 . The heavy neutrino mass m_N joins two different bispinors in the Dirac case and the same one in the Majorana one. Heavy neutrino decays are given by their interactions in Eqs. (1): $N \rightarrow W^+ \ell^-$, $N \rightarrow Z \nu$, $N \rightarrow H \nu$, plus $N \rightarrow W^- \ell^+$ for a heavy Majorana neutrino. For $m_N < M_W$ all these decays are to three body final states, mediated by off-shell W , Z or H bosons, and have been included in the heavy neutrino ALPGEN extension (see next section). The total width for a Majorana neutrino is twice larger than for a Dirac one with the same couplings [5, 12–14].

As it is apparent from Eqs. (1), heavy neutrino signals are proportional to the neutrino mixing with the SM leptons $V_{\ell N}$. Limits on these matrix elements have been extensively discussed in previous literature, and we quote here only the main results. Low-energy data constrain the quantities

$$\Omega_{\ell\ell'} \equiv \delta_{\ell\ell'} - \sum_{i=1}^3 V_{\ell\nu_i} V_{\ell'\nu_i}^* = \sum_{j=1}^n V_{\ell N_j} V_{\ell' N_j}^*. \tag{2}$$

A global fit to tree level processes involving light neutrinos as external states gives [15, 16],

$$\Omega_{ee} \leq 0.0054, \quad \Omega_{\mu\mu} \leq 0.0096, \quad \Omega_{\tau\tau} \leq 0.016 \tag{3}$$

at 90% confidence level (CL). Note that a global fit without the unitarity bounds implies $\Omega_{ee} \leq 0.012$ [15]. Additionally, for Majorana neutrinos coupling to the electron the experimental bound on neutrinoless double beta decay requires [17]

$$\left| \sum_{j=1}^n V_{eN_j}^2 \frac{1}{m_{N_j}} \right| < 5 \times 10^{-8} \text{ GeV}^{-1}. \tag{4}$$

If V_{eN_j} saturate Ω_{ee} in Eq. (3), this limit can be satisfied either demanding that m_{N_j} are large enough, beyond the TeV scale [18] and then beyond LHC reach, or that there is a cancellation among the different terms in Eq. (4), as may happen in definite models [19], in particular for (quasi)Dirac neutrinos.

Flavour changing neutral processes further restrict $\Omega_{\ell\ell'}$. The new contributions, and then the bounds, depend on the heavy neutrino masses. In the limit $m_{N_j} \gg M_W$ [20] they imply

$$|\Omega_{e\mu}| \leq 0.0001, \quad |\Omega_{e\tau}| \leq 0.01, \quad |\Omega_{\mu\tau}| \leq 0.01. \quad (5)$$

Except in the case of $\Omega_{e\mu}$, for which experimental constraints on lepton flavour violation are rather stringent, these limits are similar to the limits on the diagonal elements. An important difference, however, is that (partial) cancellations among loop contributions of different heavy neutrinos may be at work [21]. Cancellations with other new physics contributions are also possible. Since we are interested in determining the heavy neutrino discovery potential and the direct limits on neutrino masses and mixings which can be eventually established, we must consider the largest possible neutrino mixings, although they may require model dependent cancellations or fine-tuning.

3 Heavy neutrino production with ALPGEN

For the signal event generation we have extended ALPGEN [9] with heavy neutrino production. This Monte Carlo generator evaluates tree level SM processes and provides unweighted events suitable for simulation. A simple way of including new processes taking advantage of the ALPGEN framework is to provide the corresponding squared amplitudes decomposed as a sum over the different colour structures. In the case of heavy neutrinos this is trivial because there is only one term. This method requires to evaluate from the beginning the squared amplitudes for the processes one is interested in, what is done using HELAS [22]. An alternative possibility which gives more flexibility for future applications is to implement the new vertices at the same level as the SM ones, what is quite more involved.

We have restricted ourselves to single heavy neutrino production. Pair production is suppressed by an extra V^2 mixing factor and by the larger center of mass energy required, what implies smaller PDFs and more suppressed s -channel propagators. Single heavy neutrino production can proceed through s -channel W , Z or H exchange. From these, the first one $p\bar{p}^{(-)} \rightarrow W \rightarrow \ell N$ is the most interesting process for N discovery, and has been implemented in ALPGEN for the various possible final states given by the heavy neutrino decays $N \rightarrow W^\pm \ell^\mp$, $N \rightarrow Z \nu_\ell$, $N \rightarrow H \nu_\ell$ with $\ell = e, \mu, \tau$, and for both Dirac or Majorana N . In the case $m_N < M_W$ all decays are three-body, and mediated by off-shell W , Z or H . The transition from two-body to three-body decays on the M_W , M_Z and M_H thresholds is smooth, since the calculation of matrix elements and the N width are done for off-shell intermediate bosons. Two approximations are made,

however. The small mixing of heavy neutrinos with charged leptons implies that their production is dominated by diagrams with N on-shell, like those shown in Fig. 1, with a pole enhancement factor, and that non-resonant diagrams are negligible. (Additionally, to isolate heavy neutrino signals from the background one expects that the heavy neutrino mass will have to be reconstructed to some extent.) Then, the only diagrams included are the resonant ones. In the calculation we also neglect light fermion masses except for the bottom quark.

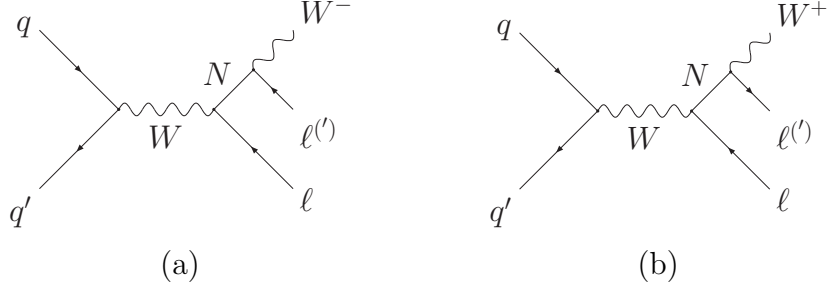


Figure 1: Feynman diagrams for the process $q\bar{q}' \rightarrow \ell^+ N$, followed by LNV decay $N \rightarrow \ell'^+ W^-$ (a) and LNC decay $N \rightarrow \ell'^- W^+$ (b). The diagrams for the charge conjugate processes are similar.

Generator-level results are presented in Fig. 2 for LHC and Tevatron in the relevant mass ranges. Solid lines correspond to the total μN cross sections for $|V_{\mu N}| = 0.098$, $V_{eN} = V_{\tau N} = 0$. The dashed lines are the cross sections for the final state $\mu^\pm \mu^\pm jj$, which is the cleanest one. The dotted lines are the same but with kinematical cuts

$$\begin{aligned}
 \text{LHC : } & p_T^\mu \geq 10 \text{ GeV}, \quad |\eta^\mu| \leq 2.5, \quad \Delta R_{\mu j} \geq 0.4, \\
 & p_T^j \geq 10 \text{ GeV}, \quad |\eta^j| \leq 2.5, \\
 \text{Tevatron : } & p_T^\mu \geq 10 \text{ GeV}, \quad |\eta^\mu| \leq 2, \quad \Delta R_{\mu j} \geq 0.4, \\
 & p_T^j \geq 10 \text{ GeV}, \quad |\eta^j| \leq 2.5,
 \end{aligned} \tag{6}$$

included to reproduce roughly the acceptance of the detector and give approximately the “effective” size of the observable signal. Of course, the correct procedure is to perform a simulation, as we do in next section, but for illustrative purposes we include the cross-sections after cuts. In particular, they clearly show that although for $m_N < M_W$ the total cross sections grow several orders of magnitude, both at LHC and Tevatron, partons tend to be produced with low transverse momenta (the two muons and two quarks result from the decay of an on-shell W), making the observable signal much smaller. These results are in agreement with those previously obtained in Ref. [4].

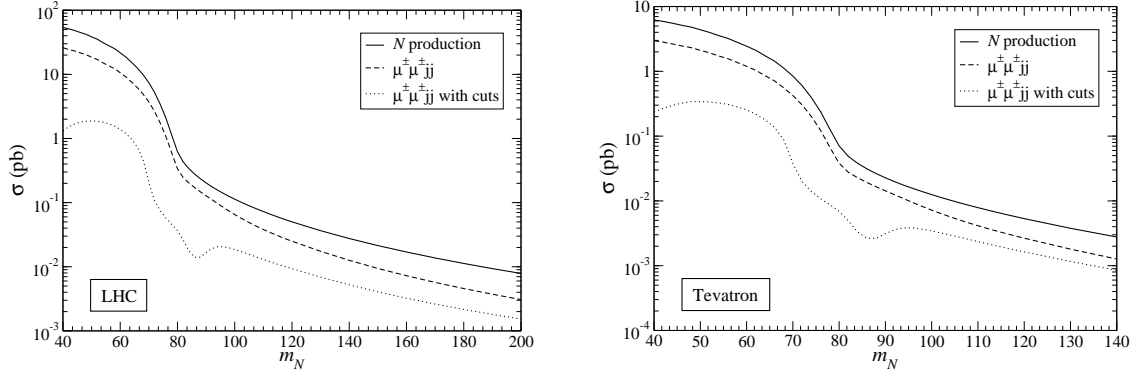


Figure 2: Cross sections for heavy neutrino production at LHC (left) and Tevatron (right), as a function of the heavy neutrino mass, for $|V_{\mu N}| = 0.098$. The solid lines correspond to total μN cross section, the dashed lines include the decay to same-sign muons and the dotted lines are the same but including the kinematical cuts in Eq. (6).

4 Di-lepton signals at LHC

We analyse in detail the case of a Majorana neutrino coupling only to the muon, which is, as it has already been emphasised, the situation in which LHC has better discovery prospects than ILC [14]. The most interesting final state is $\mu^\pm\mu^\pm jj$, with two same sign muons and at least two jets. Since this LNV signal has sometimes been considered [2, 4] to be almost background free (more realistic background estimates are given in Ref. [23]), a detailed discussion of the actual backgrounds is worthwhile. A first group of processes involves the production of additional leptons, either neutrinos or charged leptons (which may be missed in the detector). The main ones are $W^\pm W^\pm nj$ and $W^\pm Z nj$, where nj stands for $n = 0, 1, 2, \dots$ additional jets. We point out that not only the processes with $n = 2$ contribute: processes with $n < 2$ are backgrounds due to the appearance of extra jets from pile-up, and processes with $n > 2$ cannot be cleanly removed because of pile-up on the signal. A second group includes final states with b and/or \bar{b} quarks, like $t\bar{t}nj$, with semileptonic decay of the $t\bar{t}$ pair, and $Wb\bar{b}nj$, with W decaying leptonically. In these cases the additional same-sign muon results from the decay of a b or \bar{b} quark. Only a tiny fraction of such decays produce isolated muons with sufficiently high transverse momentum. But, since the $t\bar{t}nj$ and $Wb\bar{b}nj$ cross sections are so large, these backgrounds are also much larger than backgrounds with two weak gauge bosons. An important remark here is that the corresponding backgrounds $t\bar{t}nj, Wb\bar{b}nj \rightarrow e^\pm e^\pm X$ are one order of magnitude larger than the ones involving muons. The reason is that b decays produce “apparently isolated” electrons more often than muons, because electrons are detected in the calorimeter while muons

travel to the muon chamber. Hence, a reliable evaluation of the $e^\pm e^\pm X$ background resulting from these processes seems to require a full simulation of the detector. Finally, $b\bar{b}nj$ production is several orders of magnitude larger than all processes mentioned above, but the produced muons have small p_T and invariant mass in this case. Then, in general it might be eliminated with suitable high- p_T cuts on charged leptons [24] (see section 4.1), but for $m_N < M_W$ the heavy neutrino signal is also characterised by very small transverse momenta (see section 4.2), and this background turns out to be the dominant one.

We have generated the signal and backgrounds using ALPGEN and passing them through PYTHIA 6.4 [25] with the MLM prescription [26] to avoid double counting of jet radiation. A fast simulation of the ATLAS detector [27] has been performed. For the signal and all backgrounds except $b\bar{b}nj$ the number of simulated events corresponds to 10 times the luminosity considered (which is 30 fb^{-1}), so as to reduce statistical fluctuations. For $b\bar{b}nj$ this is not possible. The $b\bar{b}$ cross section is $1.5 \text{ } \mu\text{b}$ when both b quarks are required to have $p_T^b \geq 20 \text{ GeV}$ at the generator level. Fast simulation of 30 fb^{-1} would take about 15000 days in a modern single-processor system, making this computation difficult even in multi-processor grids. (Full simulation would take about 10^6 years, and in the real experiment this background must be estimated from data, as it has been done by D0 [28].) Therefore, we have simulated samples of 100, 40, 20 and 10 million events for $b\bar{b}$, $b\bar{b}j$, $b\bar{b}2j$ and $b\bar{b}3j$, respectively, corresponding to luminosities $L = 69.9, 102.7, 167.1$ and 345 pb^{-1} . The number of events at pre-selection is calculated by rescaling the number of events to 30 fb^{-1} ,

$$N(\mu^\pm \mu^\pm; \text{pre}, 30) \simeq N(\mu^\pm \mu^\pm; \text{pre}, L) f_L, \quad (7)$$

with factors $f_L = 429, 292, 179$ and 87 for each of the $b\bar{b}nj$, $n = 0 - 3$ processes. However, the estimation of the number of events after selection cuts cannot be done in this way, since no $\mu^\pm \mu^\pm$ events survive the cuts applied. Instead, we make the reasonable assumption that selection cuts, which are based on kinematical variables, have the same effect on all $\ell\ell'$ events, where $\ell, \ell' = e, \mu$, not necessarily of the same charge. Then, for $b\bar{b}nj$ backgrounds the number of $\mu^\pm \mu^\pm$ events after selection cuts for 30 fb^{-1} can be estimated from the samples with a smaller luminosity L as

$$N(\mu^\pm \mu^\pm; \text{sel}, 30) \simeq N(\ell\ell'; \text{sel}, L) \left[\frac{N(\mu^\pm \mu^\pm; \text{pre}, L)}{N(\ell\ell'; \text{pre}, L)} f_L \right]. \quad (8)$$

Since the numbers of $\ell\ell'$ events for the different $b\bar{b}nj$ processes are about $150 - 300$ times larger than the numbers of $\mu^\pm \mu^\pm$ events, the term in brackets in Eq. (8) is of order unity, and thus the simulated samples provide a good estimate of the results for $\mu^\pm \mu^\pm$ final states. It is worth remarking here that raising the p_T^b threshold at generator level,

e.g. to 50 GeV, leads to a dramatic reduction of the $b\bar{b}nj$ cross sections (by factors of 24 and 17 for $b\bar{b}$ and $b\bar{b}j$, respectively), making the simulation more manageable. However, this also results in a gross underestimation of the $b\bar{b}nj$ background. We have checked this by simulating two samples of 25 million $b\bar{b}$ events with $p_T^b \geq 20$ and $p_T^b \geq 50$ GeV, respectively, and two samples of 10 million $b\bar{b}j$ events with the same generator-level cuts. For pre-selection we just require two isolated muons of either charge with $p_T^\mu \geq 10$ GeV. For the $p_T^b \geq 20$ samples we obtain 364 $b\bar{b} \rightarrow \mu\mu$ and 115 $b\bar{b}j \rightarrow \mu\mu$ events. For the $p_T^b \geq 50$ samples we only obtain 287 and 55 events, respectively. Hence, given the difference in cross sections indicated above, raising p_T^b to 50 GeV at event generation would underestimate these two backgrounds by factors of 30 and 35. This seems to be related to the fact that b quarks with larger transverse momentum give more collimated decay products, and thus the muons are less isolated. On the other hand, b quarks with too low transverse momentum cannot produce muons with $p_T^\mu \geq 10$ GeV. For this reason, we expect that our evaluation of $b\bar{b}nj$ provides a good estimate of the actual background to be found at LHC. The contribution from $c\bar{c}nj$ has been neglected here because c quarks give less isolated charged leptons, but eventually will have to be included when confronting real data.

4.1 $\mu^\pm\mu^\pm jj$ production for $m_N > M_W$

In this mass region we take the reference values $m_N = 150$ GeV and $V_{\mu N} = 0.098$. The pre-selection criteria used for our analysis are:

- (i) two same-sign isolated muons with pseudorapidity $|\eta^\mu| \leq 2.5$ and transverse momentum p_T^μ larger than 10 GeV, and no additional isolated charged leptons;
- (ii) no additional non-isolated muons;
- (iii) two jets with $|\eta^j| \leq 2.5$ and $p_T^j \geq 20$ GeV.

We note that the requirement (ii) reduces the backgrounds involving Z bosons by almost a factor of two, and thus proves to be quite useful. The number of events at LHC for 30 fb^{-1} after pre-selection cuts is given in Table 1. Additional backgrounds such as $t\bar{t}4j$, $t\bar{t}5j$, $ZZnj$, $WWZnj$, $WZZnj$, $ZZZnj$ are smaller and we do not show them, but they are included in the estimation of the signal significance below. Single top production is very small, and included only for comparison with existing analyses.

The fast simulation shows that SM backgrounds are about two orders of magnitude larger than previously estimated (three orders if we include $b\bar{b}nj$). Moreover, they

	Pre-selection				Selection			
	$n = 0$	$n = 1$	$n = 2$	$n = 3$	$n = 0$	$n = 1$	$n = 2$	$n = 3$
μN	92.9	—	—	—	38.3	—	—	—
$b\bar{b}nj$	13700	7600	3400	610	0	0	0	0
$t\bar{t}nj$	747.8	730.3	405.0	240.9	0.9	0.3	0.3	0.0
$Wb\bar{b}nj$	53.9	254.9	232.5	222.5	0.0	0.1	0.2	0.1
$Zb\bar{b}nj$	12.5	27.5	14.8	13.0	0.0	0.0	0.0	0.0
$WWnj$	×	×	116.2	200.2	×	×	1.5	0.8
$WZnj$	57.7	156.1	244.8	156.9	0.2	0.9	2.9	0.8
$WWWnj$	13.3	23.8	26.8	18.4	0.2	0.5	0.0	0.0
tnj	×	62.0	—	—	×	0.2	—	—
$t\bar{b}nj$	3.5	—	—	—	0.0	—	—	—

Table 1: Number of $\mu^\pm\mu^\pm X$ events at LHC for 30 fb^{-1} , at the pre-selection and selection levels. The heavy neutrino signal is evaluated assuming $m_N = 150\text{ GeV}$ and $V_{\mu N} = 0.098$. Processes which do not contribute are marked with a cross. Signal contributions with extra jets not available at the generator level are marked with a dash.

cannot be sufficiently suppressed with respect to the heavy neutrino signal using simple cuts. Some obvious discriminating variables are:

- The missing momentum \cancel{p}_T . It is smaller for the signal because it does not have neutrinos in the final state.
- The separation between the muon with smallest p_T (we label the two muons as μ_1, μ_2 , by decreasing transverse momentum) and the closest jet, $\Delta R_{\mu_2 j}$. For backgrounds involving high- p_T b quarks this separation tends to be rather small.
- The transverse momentum of the two muons, $p_T^{\mu_1}$ and $p_T^{\mu_2}$, respectively. In particular $p_T^{\mu_2}$ is a good discriminant against backgrounds from b quarks, because these typically have one muon with small p_T .

These variables are plotted in Fig. 3 for the signal and the two background groups which turn out to be relevant: those where one muon comes from a b quark (that is, $t\bar{t}nj$ and $W/Zb\bar{b}nj$ but not $b\bar{b}nj$) and those where both muons come from W/Z decays (that is, di-boson and tri-boson production). Kinematical cuts on them do not render the $\mu^\pm\mu^\pm jj$ final state “background free”, as it is apparent from the plots (and we have explicitly checked). Indeed, for the large background cross sections in Table 1 the overlapping regions contain a large number of background events, and they can only be

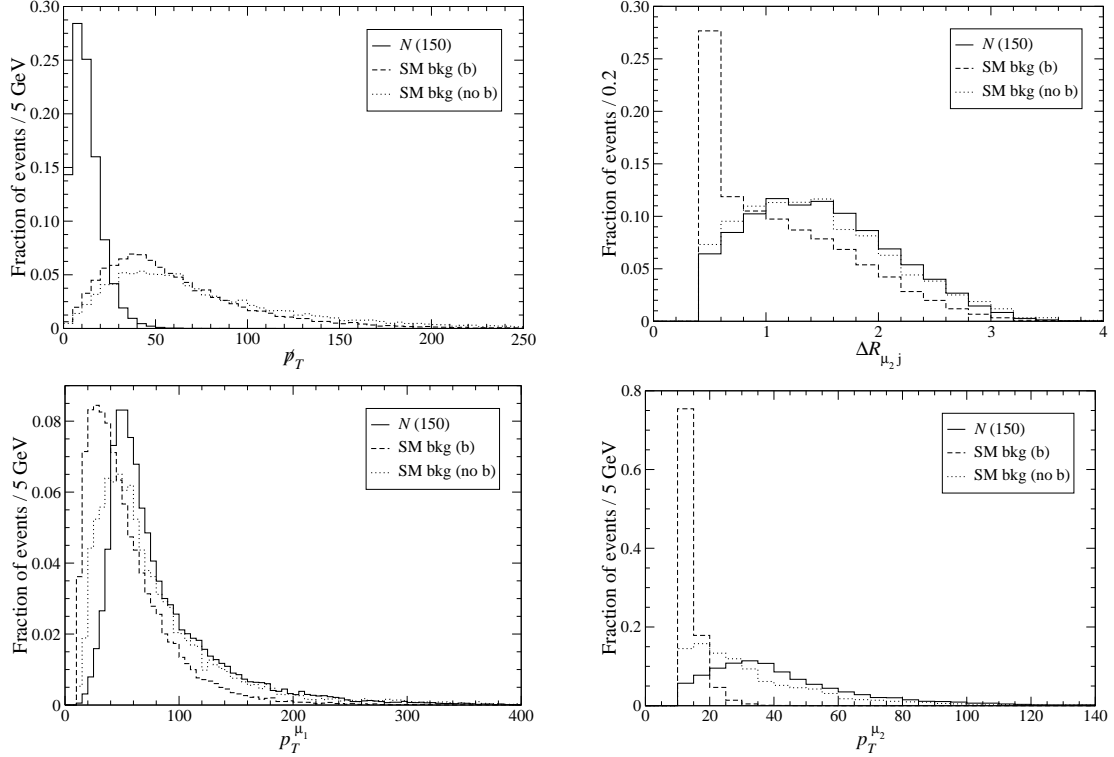


Figure 3: Normalised distributions of several discriminating variables for the $m_N = 150$ GeV signal and the backgrounds with and without a muon from a b quark, excluding $b\bar{b}n j$ (see the text).

eliminated by severely reducing the signal. However, a likelihood analysis using these and several other variables can efficiently reduce the background. Additional relevant variables are shown in Fig. 4:

- The invariant mass of μ_2 (the muon with lowest p_T) and the two jets which best reconstruct the W boson,¹ $m_{W\mu_2}$. An important observation in this case is that in backgrounds involving b quarks this muon typically has a small p_T , displacing the background peak to lower invariant masses.
- The invariant mass of the two muons.

¹The reconstruction of the W boson from two jets is done trying all possible pairings among the four jets with maximum p_T . This is done to ensure a good reconstruction of the heavy neutrino mass in the presence of pile-up, which gives several additional jets in each event and prevents from reconstructing the W naively, *e.g.* using the two jets with highest p_T . Although this procedure provides a good m_N reconstruction, the W reconstructed mass is no longer a useful discriminating variable. Indeed, background events quite often have two jets with invariant mass $\sim M_W$. In order to further improve the reconstruction, the two jet momenta are rescaled so that their invariant mass coincides with M_W .

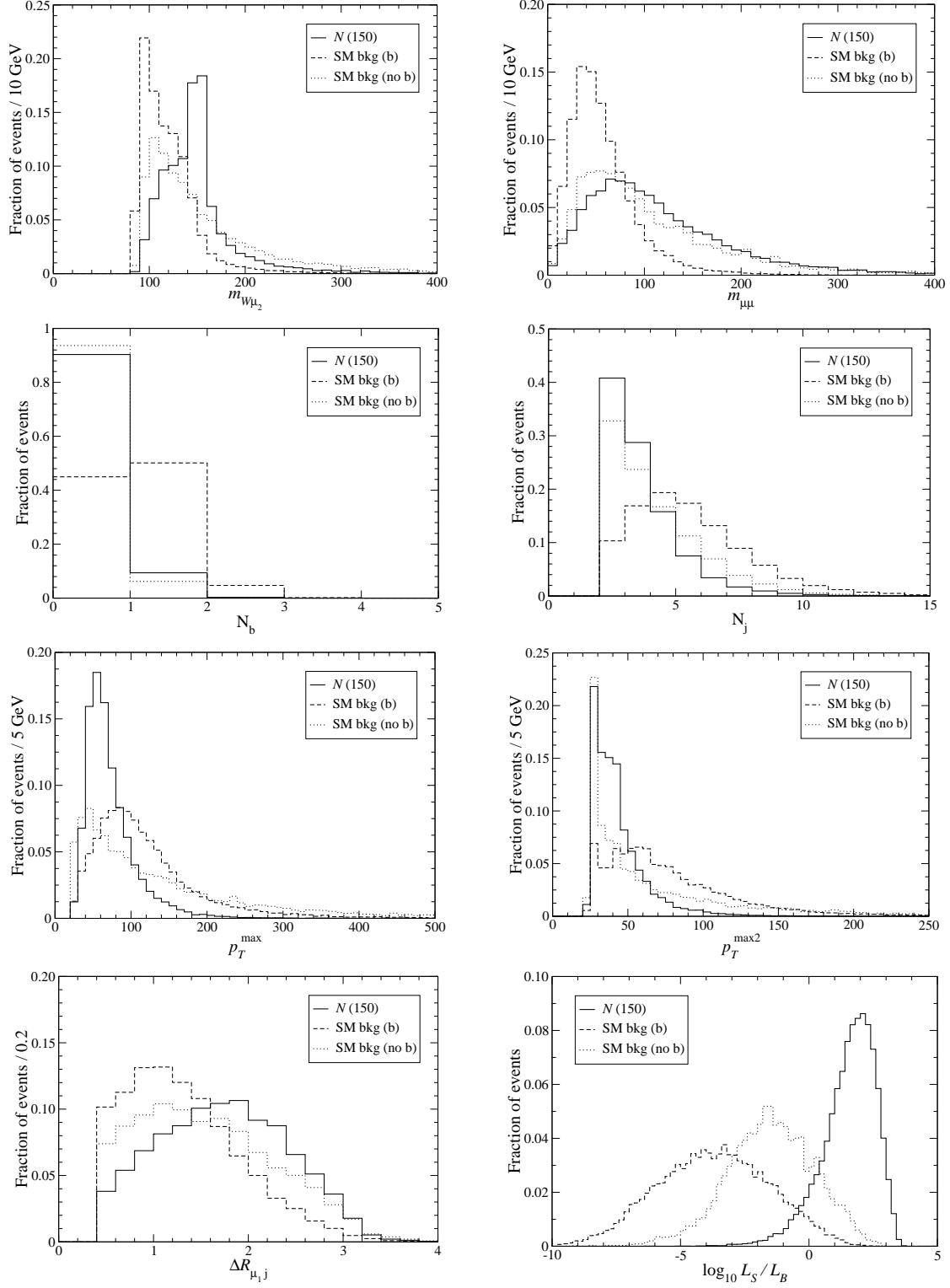


Figure 4: Normalised distributions of several discriminating variables for the $m_N = 150$ GeV signal and the backgrounds with and without a muon from a b quark, excluding $b\bar{b}nj$ (see the text). The last plot corresponds to the log-likelihood function.

- The number of b -tagged jets N_b and jet multiplicities N_j . Especially the former helps to separate the backgrounds involving b quarks because they often have b -tagged jets. In this fast simulation analysis we have fixed the b -tagging efficiency to 60%, but in a full simulation the b tag probability can be included in the likelihood function, improving the discriminating power of this variable.
- The transverse momenta of the jet with maximum and second maximum p_T , respectively p_T^{\max} and $p_T^{\max 2}$.
- The separation between the muon with largest p_T and the closest jet, $\Delta R_{\mu_1 j}$.

These variables are not suited for performing kinematical cuts but greatly improve the discriminating power of a likelihood function. Three additional variables, less important and hence not shown for brevity, are the angles between the W and the muons and the pseudorapidity of the muon which best reconstructs the heavy neutrino mass. The resulting log-likelihood function is also shown in Fig. 4, where we distinguish three likelihood classes as in the previous figures: the signal, backgrounds with one muon from b decays, and backgrounds with both muons from W/Z decays. $b\bar{b}nj$ is not included in the likelihood analysis because it is not necessary: it can be efficiently suppressed already with the kinematical distributions used to reduce the remaining backgrounds.

As selection criteria we require $\log_{10} L_S/L_B \geq 1.75$ and that at least one of the two heavy neutrino mass assignments $m_{W\mu_1}, m_{W\mu_2}$ is between 130 and 170 GeV.² The number of events surviving these cuts can be read on the right part of Table 1. As it is apparent, the likelihood analysis is quite effective in suppressing backgrounds, especially $b\bar{b}nj$, $t\bar{t}nj$ and $W/Zb\bar{b}nj$. Assuming a “reference” 20% systematic uncertainty in the backgrounds (which still has to be precisely evaluated), the resulting statistical significance for the heavy neutrino signal is of 9.9σ . A 150 GeV heavy neutrino can be discovered for mixings $|V_{\mu N}| \geq 0.07$, and if no background excess is found the limits $|V_{\mu N}|^2 \leq 1.6 (1.9) \times 10^{-3}$ can be set at 90% (95%) CL. Heavy neutrino masses up to 175 GeV can be observable with 5σ at the LHC for $V_{\mu N} = 0.098$. These figures can be considered conservative because only the lowest-order signal contribution (without hard extra jets at the partonic level) has been included, and further signal contributions $\mu N nj$ should improve the heavy neutrino observability. If the Higgs is heavier

²The latter requirement assumes a previous knowledge of m_N , in the same way as the signal distributions for the likelihood analysis are built for a precise m_N value. Thus, experimental searches must be performed by comparing data with Monte-Carlo samples generated for different values of m_N . This procedure, although more involved than a search with generic cuts, provides much better sensitivity.

than 120 GeV the branching ratio $\text{Br}(N \rightarrow W\mu)$ will increase as well.

4.2 $\mu^\pm\mu^\pm jj$ production for $m_N < M_W$

In this mass region we take the reference values $m_N = 60$ GeV and $V_{\mu N} = 0.01$. The pre-selection criteria are the same as before. The likelihood analysis is performed distinguishing four classes; in addition to the three ones considered for $m_N = 150$ GeV we now include $b\bar{b}nj$. The relevant variables are depicted in Figs. 5 and 6:

	Pre-selection				Selection			
	$n = 0$	$n = 1$	$n = 2$	$n = 3$	$n = 0$	$n = 1$	$n = 2$	$n = 3$
μN	383.9	—	—	—	32.5	—	—	—
$b\bar{b}nj$	13700	7600	3400	610	5.6	4.0	3.4	0
$t\bar{t}nj$	747.8	730.3	405.0	240.9	0.0	0.0	0.0	0.0
$Wb\bar{b}nj$	53.9	254.9	232.5	222.5	0.0	0.0	0.1	0.0
$Zb\bar{b}nj$	12.5	27.5	14.8	13.0	0.0	0.0	0.0	0.0
$WWnj$	×	×	116.2	200.2	×	×	0.0	0.0
$WZnj$	57.7	156.1	244.8	156.9	0.2	0.2	0.1	0.0
$WWWnj$	13.3	23.8	26.8	18.4	0.0	0.0	0.0	0.0
tnj	×	62.0	—	—	×	0.0	—	—
$t\bar{b}nj$	3.5	—	—	—	0.0	—	—	—

Table 2: Number of $\mu^\pm\mu^\pm X$ events at LHC for 30 fb^{-1} , at the pre-selection and selection levels. The heavy neutrino signal is evaluated assuming $m_N = 60$ GeV and $V_{\mu N} = 0.01$. Processes which do not contribute or are absent are marked with a cross. Signal contributions with extra jets not available at the generator level are marked with a dash.

- The transverse momenta of the two muons (slightly smaller for $b\bar{b}nj$ than for the signal, and much larger for the other backgrounds).
- The distance between them and the closest jet, which is a good discriminator against $t\bar{t}nj$ but not against $b\bar{b}nj$.
- The rapidity difference between the muons and the W^* from N decay, which is reconstructed from the two jets with highest p_T .

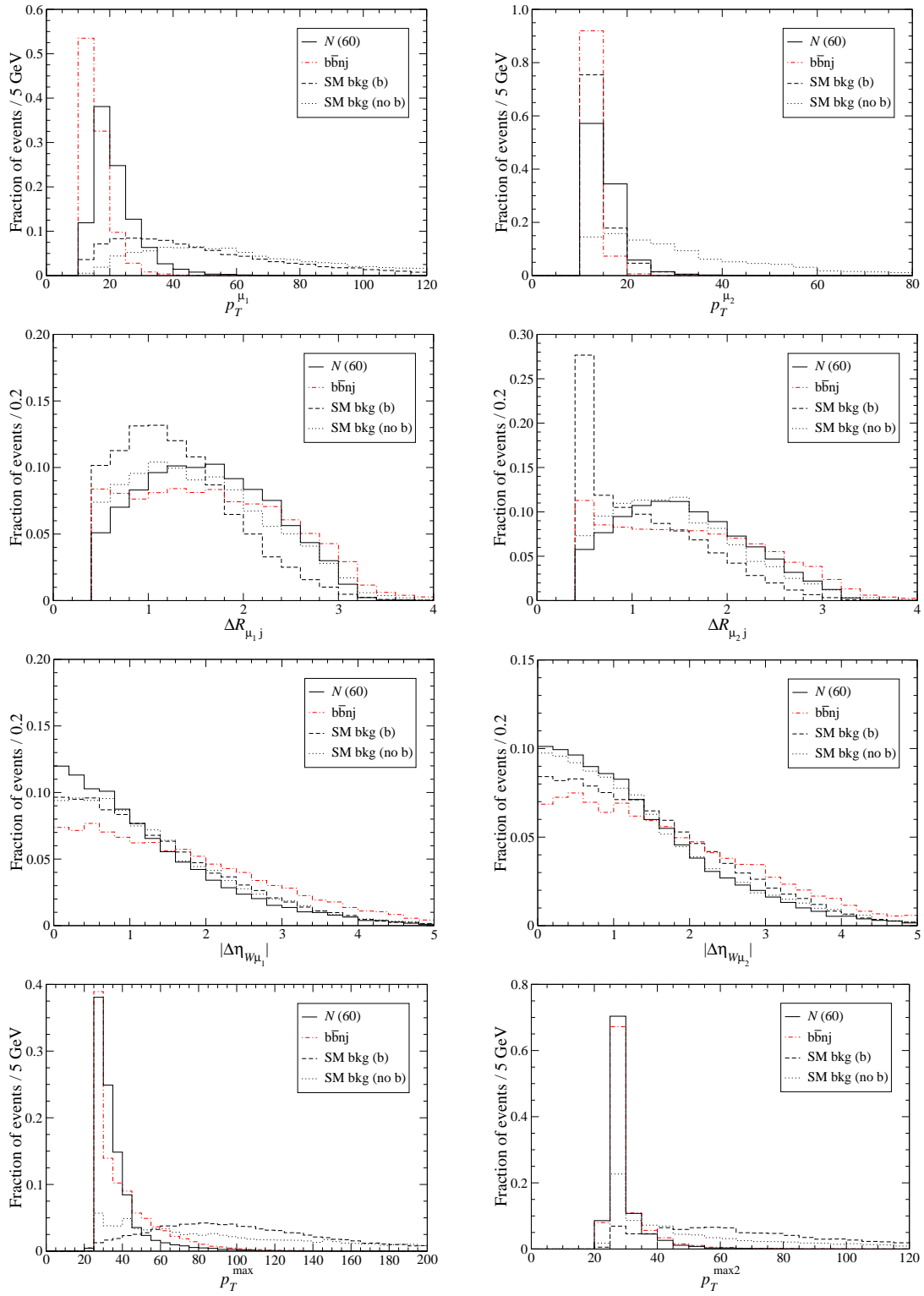


Figure 5: Normalised distributions of several discriminating variables for the $m_N = 60$ GeV signal and the three background classes (see the text).

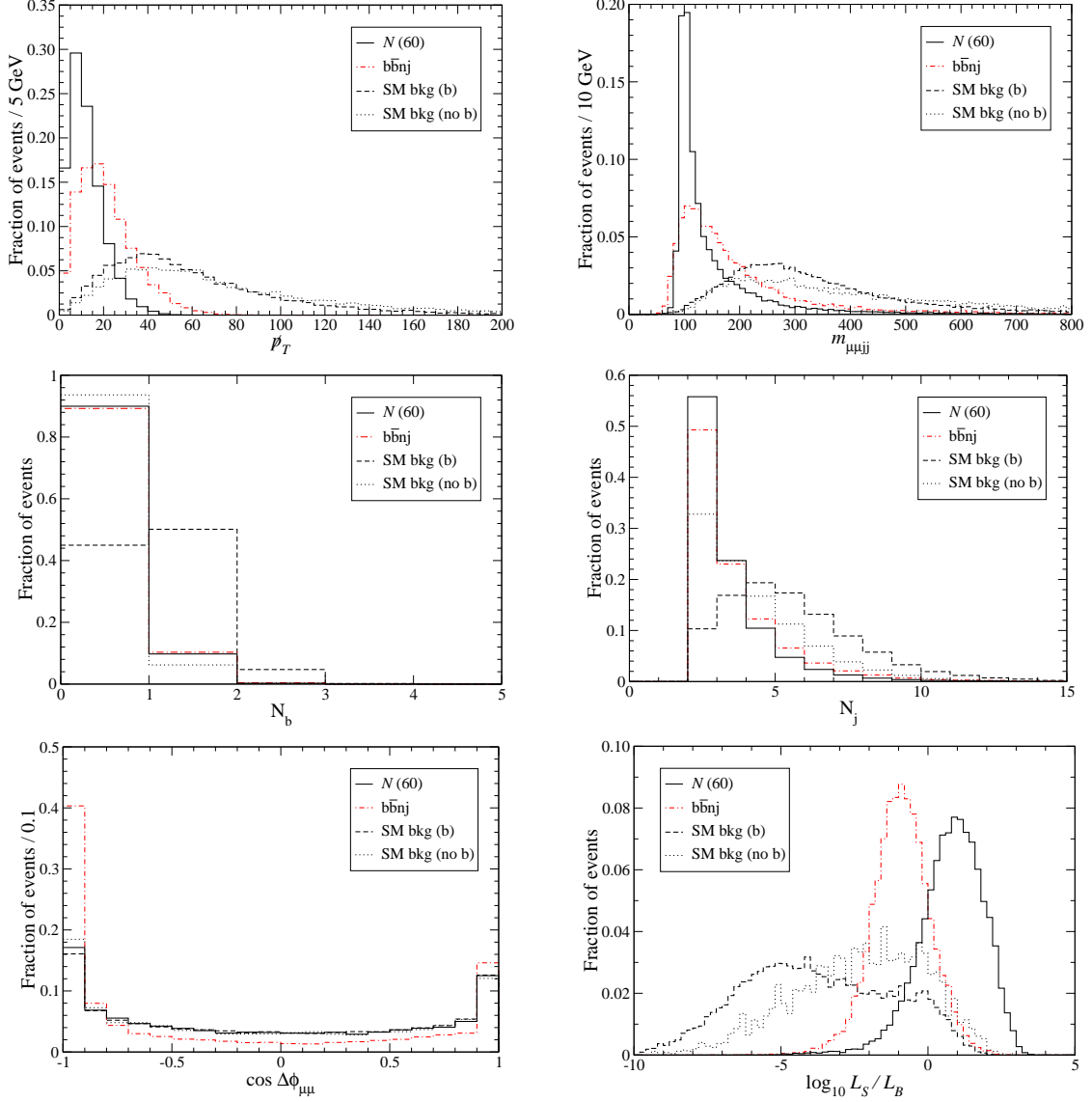


Figure 6: Normalised distributions of several discriminating variables for the $m_N = 60$ GeV signal and the three background classes (see the text). The last plot corresponds to the log-likelihood function.

- The transverse momenta of the two jets with largest p_T . Again, these two variables are excellent discriminators against high- p_T backgrounds like $t\bar{t}nj$ and diboson production, but not very useful for $b\bar{b}nj$.
- The missing transverse momentum.
- The invariant mass of the two muons and two jets with highest p_T , $m_{\mu jj}$. For the signal, these four particles result from the decay of an on-shell W boson,

so the distribution is very peaked around 100 GeV (the position of the peak is displaced as a consequence of pile-up, which generates jets with larger p_T than the ones from the signal itself). Unfortunately, for $b\bar{b}nj$ the distribution is quite similar.

- The number of b tags and the jet multiplicity.
- The azimuthal angle (in transverse plane) between the two muons, $\phi_{\mu\mu}$. For $b\bar{b}$ without additional jets this angle is often close to 180° , but for $b\bar{b}j$ and higher order processes (which are also huge) this no longer holds.

The resulting log-likelihood function is presented in Fig. 6. As it can be easily noticed with a quick look at the variables involved, $b\bar{b}nj$ production has a topology very similar to the signal and is very difficult to eliminate. Requiring a strict cut $\log_{10} L_S/L_B \geq 2.2$ practically eliminates all backgrounds except this one, as it can be observed in the right part of Table 2 (numbers of background events at pre-selection are equal to the ones in Table 1 and quoted for better comparison). With this selection cut the statistical significance of the signal is 7.1σ . A 60 GeV neutrino can be discovered for mixings $|V_{\mu N}| \geq 0.0084$, and bounds $|V_{\mu N}|^2 \leq 2.4(2.8) \times 10^{-5}$ can be set at 90% (95%) CL if a background excess is not observed. These figures are ~ 50 times worse than in previous parton-level estimates [4] which overlooked the main background $b\bar{b}nj$, but would still improve the direct limit from L3 [29, 30] by an order of magnitude.

Since present limits from L3 still allow for discovering a heavy neutrino in this mass range (and also for $m_N \geq M_W$, where these limits are much less restrictive), one may wonder how its mass could be determined. For $m_N \geq M_W$ this would be straightforward, as seen in the first plot of Fig. 4, because the W boson from $N \rightarrow W\mu$ is produced on its mass shell and the two jets from its decay have in general large transverse momentum. For $m_N \leq M_W$, however, it is very difficult to identify the two jets coming from $N \rightarrow W^*\mu$, which have low transverse momenta, in the presence of pile-up. One possibility for the mass determination could be to consider the invariant mass of the two muons, which we present in Fig. 7 (left) for heavy neutrino masses of 50, 60 and 70 GeV. This distribution seems to peak around $m_N/2$. Other possibility is to exploit the fact that, since the on-shell decay $W \rightarrow \mu N$ is two-body, the energy of *this* muon in the centre of mass (CM) system, E_μ^{CM} , is fixed by m_N . Thus, we may determine the heavy neutrino mass as

$$m_N^{\text{CM}} = \sqrt{M_W^2 - 2M_W E_\mu^{\text{CM}}}. \quad (9)$$

The m_N reconstruction from the muon energy in CM frame (defined as the rest frame of the two muons and two jets with largest p_T) is shown in Fig. 7 (right). For each event

two values of m_N^{CM} are calculated, for each one of the muons, and both are plotted. Imaginary values are discarded. Both two procedures for m_N determination will be subject to possibly large systematic uncertainties, but their evaluation is beyond the scope of this work. (For example, the reconstruction from muon energy in CM frame is expected to have a systematic uncertainty from pile-up, which could be decreased using the muon energies in the laboratory frame, but at the expense of losing sensitivity to m_N .) If heavy neutrinos were discovered, interesting information about CP violation, relevant for leptogenesis, could also be inferred [31],

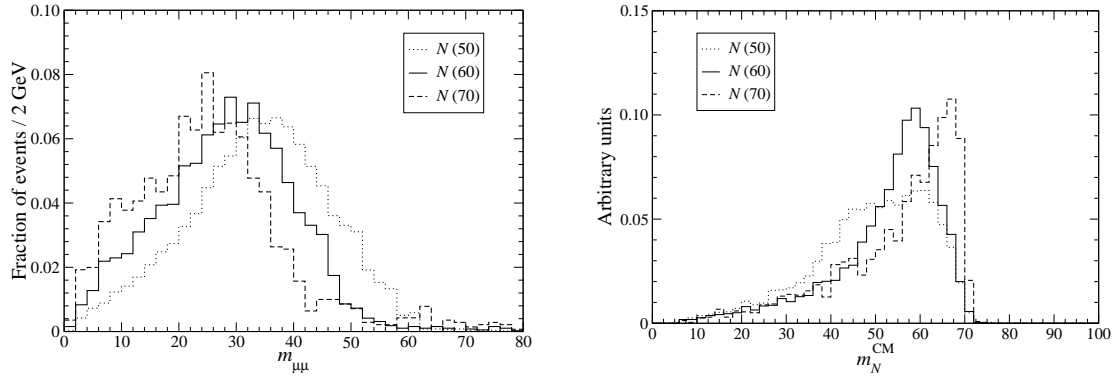


Figure 7: Left: invariant mass of the two muons, for three heavy neutrino masses. Right: heavy neutrino mass reconstructed from the muon energy in CM frame.

4.3 Other same-sign dilepton signals

In final states $e^\pm e^\pm$, $e^\pm \mu^\pm$ the analysis is similar but the backgrounds are larger, as it has been pointed out before. In fact, it seems likely that a reliable estimation of the $e^\pm e^\pm$, $e^\pm \mu^\pm$ backgrounds from $t\bar{t}nj$ and $W/Zb\bar{b}nj$ production requires a very good knowledge of the detector, that is, a full simulation. However, with the results in section 4.1 one may still attempt to provide approximate limits for these two channels, before a complete and lengthy analysis is done.

For a heavy neutrino coupling only to the electron we assume a reference value $V_{eN} = 0.073$ and $V_{\mu N} = V_{\tau N} = 0$, and consider $e^\pm e^\pm$ final states. We take the $t\bar{t}nj$, $W/Zb\bar{b}nj$ backgrounds as ten times larger than the corresponding ones involving muons, as it is found with fast detector simulation. The $ZWnj$ ones are estimated to be 1.7 times larger, corresponding to the effect of the pre-selection requirement of no non-isolated muons, which has no analogous for electrons. The $WWnj$ and $WWWnj$ backgrounds should be of the same size. With this rescaling of the backgrounds in

Table 1 and the mass dependence of the cross sections in Fig. 2, we estimate that for $V_{eN} = 0.073$ it is possible to have 5σ significance up to masses $m_N \simeq 130$ GeV.

For a heavy neutrino coupling to both electron and muon, we assume for definiteness $V_{eN} = 0.073$, $V_{\mu N} = 0.098$, $V_{\tau N} = 0$ (see section 2, however). The procedure followed to extract limits is the same, but considering the various production and decay possibilities. Adding the statistical significances of the three channels $e^\pm e^\pm$, $\mu^\pm \mu^\pm$ and $e^\pm \mu^\pm$, and rescaling from the cross sections in Fig. 2, we find 5σ significance up to masses $m_N \simeq 160$ GeV. We do not address the observability of heavy neutrino signals in τ lepton channels, which are expected to have much worse sensitivity. For hadronic τ decays the charge of the decaying lepton seems rather difficult to determine, hence backgrounds from $Z \rightarrow \tau^+ \tau^-$ will be huge. For leptonic decays $\tau \rightarrow \ell \nu_\tau \bar{\nu}_\ell$, $\ell = e, \mu$, not only the branching ratios are smaller, but also the signal has final state neutrinos and thus the discriminating power of \cancel{p}_T against di-boson and tri-boson backgrounds is much worse.

5 Estimates for Tevatron

The observability of heavy neutrino signals in same-sign dilepton channels at Tevatron seems to be dominated by the size of the signal itself. In contrast with LHC, backgrounds are much smaller. For example, the $WZjj$ and $WWjj$ backgrounds have cross sections of 0.1 and 0.09 fb, respectively, with the cuts in Eq. (6). Then, it seems reasonable to estimate the total background for 1 fb^{-1} (including $b\bar{b}$) as one event. This rough estimation is in agreement with the detailed calculation in Ref. [28], in which $b\bar{b}$ is estimated from real data. Therefore, if signal events have not been observed with the already collected luminosity, upper limits of 3.36 and 4.14 events [32] can be set on the signal, at 90% and 95% CL, respectively. From Fig. 2, and for a fixed mass $m_N = 60$ GeV, this implies upper bounds $|V_{\mu N}|^2 \leq 1.3 \times 10^{-4}$ (90% CL) $|V_{\mu N}|^2 \leq 1.6 \times 10^{-4}$ (95% CL). This would slightly improve the limits from L3 [29, 30]. Of course, a detailed simulation with the already collected data is necessary to make any claim, and the limits eventually obtained will depend on the actual number of observed same-sign dilepton events.

Note also that, given the cross sections in Fig. 2, for a luminosity of 1 fb^{-1} and $V_{\mu N} = 0.098$ the heavy neutrino signals only exceed one event for heavy neutrino masses $m_N < M_W$, thus the Tevatron sensitivity is limited to this mass range.

6 Conclusions

Large hadron colliders are not in principle the best place to search for new heavy neutral leptons. However, Tevatron is performing quite well and LHC will start operating soon, so one must wonder if the large electroweak rates available at large hadron colliders allow to discover new heavy neutrinos, given the present constraints on them, or improve these constraints. This is indeed the case in models with extra interactions [7,8]. In this work we have, however, assumed that no other interactions exist and that heavy neutrinos couple to the SM particles through its small mixing with the known leptons.

Heavy Dirac or Majorana neutrinos with a significant coupling to the electron can be best produced and seen at e^+e^- colliders in $e^+e^- \rightarrow N\nu \rightarrow \ell W\nu$, which has a large cross section and whose backgrounds have a moderate size [12, 14, 21, 33]. On the contrary, a Majorana N mainly coupling to the muon is easier to discover at a hadronic machine like LHC, in the process $q\bar{q}' \rightarrow W^+ \rightarrow \mu^+N$ with subsequent decay $N \rightarrow \mu^+W \rightarrow \mu^+q\bar{q}'$ (plus the charge conjugate). However, even this LNV final state is not easy to deal with. SM backgrounds are large and require a careful analysis, especially those involving b quarks, for example $b\bar{b}nj$ and $t\bar{t}nj$ which are the largest ones.

For the simulation of the $\mu^\pm\mu^\pm jj$ signal process (and other heavy neutrino decay channels which have not been studied in detail here) we have implemented heavy neutrino production in the ALPGEN framework. We have then shown, using a fast detector simulation, that a heavy neutrino with a mixing $V_{\mu N} = 0.098$ can be discovered with a 5σ significance up to masses $m_N = 175$ GeV. In the region $m_N < M_W$ we have shown that a 60 GeV neutrino can be discovered for mixings $|V_{\mu N}| \geq 0.0084$; upper limits $|V_{\mu N}|^2 \leq 2.4(2.8) \times 10^{-5}$ can be set at 90% (95%) CL if a background excess is not observed. These figures are in sharp contrast with previous estimates, and correspond to the increase in the background evaluation of about two orders of magnitude (three for $m_N < M_W$). Special care has to be taken with $b\bar{b}$ plus jets. The probability of a $b\bar{b}$ pair to give two same-sign isolated muons is tiny, but on the other hand the $b\bar{b}$ cross section $\sim 1 \mu\text{b}$ is huge. A reliable background calculation requires solving this $0 \cdot \infty$ indetermination, what is a computationally very demanding task in which some apparently reasonable simplifying assumptions, like requiring high transverse momenta of b quarks at generator level, can result in an underestimation by a factor of 30. The $b\bar{b}nj$ background has been found to be negligible for larger m_N values but dominant for $m_N \leq M_W$ (after cuts, 20 times larger than the sum of the other backgrounds). This behaviour is due to the very different signal kinematics in these two cases, with

the signal concentrated on very low transverse momenta for $m_N < M_W$.

In the two detailed analyses presented for $m_N = 150$ GeV and $m_N = 60$ GeV, we have shown that background suppression ($t\bar{t}nj$ and diboson production in the former case, $b\bar{b}nj$ in the latter) is not efficient with simple kinematical cuts, and requires more sophisticated methods, like the likelihood analysis applied here, or neural networks. The analysis could be further improved when one includes other variables not accessible at the level of fast simulation. For example, a $b\bar{b}$ pair giving two same-sign isolated muons requires the oscillation of one of the B mesons before decay. This should appear as a secondary vertex, which could be identified in the detector. On the other hand, the possibility of lepton charge misidentification should be addressed. Full simulation of $b\bar{b}nj$ for the LHC luminosity is beyond reach of present and foreseeable computers, so this background will have to be estimated from data. In any case, we stress that $b\bar{b}nj$, as well as $t\bar{t}nj$, must always be considered as a potentially dangerous source of two same-sign dileptons. And, if a moderate background excess is observed at low transverse momenta, a precise evaluation of the $b\bar{b}nj$ background is compulsory before drawing any conclusion.

Based on our detailed calculation for the $\mu^\pm\mu^\mp jj$ final state, we have estimated that a heavy neutrino only coupling to the electron with $V_{eN} = 0.073$ can be discovered up to $m_N = 130$ GeV. For a neutrino coupling simultaneously to both electron and muon, taking for reference the values $V_{\mu N} = 0.098$, $V_{eN} = 0.073$, $V_{\tau N} = 0$, the limit would be about $m_N = 160$ GeV. LNC final states have larger backgrounds, for example, $e^\pm\mu^\mp jj$ (for which $t\bar{t}nj$ is much more dangerous) and especially when lepton flavour is also conserved, as in $\mu^\pm\mu^\mp jj$. Hence, LHC is not expected to provide any useful direct limit on heavy Dirac neutrinos, for which all final states conserve lepton number. By the same token, other decay channels such as $N \rightarrow Z\nu$, $N \rightarrow H\nu$ and production processes as $pp \rightarrow Z \rightarrow N\nu$, have too large backgrounds as well.

It is finally worth noting that heavy neutrino decays, as for any other vector-like fermion, are a source of Higgs bosons [34]. Nevertheless, in contrast with the quark sector [35] Higgs boson production from N decays is rather small, and only a handful of $\mu N \rightarrow \mu\nu H \rightarrow \mu\nu b\bar{b}$ events are expected to be found at LHC. Besides, we also point out that large effects due to heavy neutrinos and, more generally, other neutrino physics beyond the SM might be observed at large hadron colliders. However, in all cases they require new interactions and often model dependent constraints. This means further assumptions, and in this situation the main novel ingredient is not only the heavy neutrino. In this category there are many interesting scenarios, also including supersymmetry (see for an example Refs. [36,37]). Then, compared to these new physics models the limits established in this work are modest. For example, if

the heavy neutrino has an interaction with a typical gauge strength, as in the case of left-right models with a new heavy W_R , the LHC reach for m_N increases up to approximately 2 TeV [7, 8].

Acknowledgements

This work has been supported by MEC project FPA2006-05294, Junta de Andalucía projects FQM 101 and FQM 437, MIUR under contract 2006020509_004, and by the European Community's Marie-Curie Research Training Network under contract MRTN-CT-2006-035505 "Tools and Precision Calculations for Physics Discoveries at Colliders". J.A.A.-S. acknowledges support by a MEC Ramón y Cajal contract.

References

- [1] A. Datta, M. Guchait and A. Pilaftsis, Phys. Rev. D **50** (1994) 3195 [arXiv:hep-ph/9311257].
- [2] F. M. L. Almeida, Y. A. Coutinho, J. A. Martins Simoes and M. A. B. do Vale, Phys. Rev. D **62** (2000) 075004 [arXiv:hep-ph/0002024].
- [3] O. Panella, M. Cannoni, C. Carimalo and Y. N. Srivastava, Phys. Rev. D **65** (2002) 035005 [arXiv:hep-ph/0107308].
- [4] T. Han and B. Zhang, Phys. Rev. Lett. **97** (2006) 171804 [arXiv:hep-ph/0604064].
- [5] F. del Aguila, J. A. Aguilar-Saavedra and R. Pittau, J. Phys. Conf. Ser. **53** (2006) 506 [arXiv:hep-ph/0606198].
- [6] P. Langacker, R. W. Robinett and J. L. Rosner, Phys. Rev. D **30** (1984) 1470.
- [7] A. Ferrari *et al.*, Phys. Rev. D **62** (2000) 013001.
- [8] S. N. Gninenko, M. M. Kirsanov, N. V. Krasnikov and V. A. Matveev, CMS-NOTE-2006-098
- [9] M. L. Mangano, M. Moretti, F. Piccinini, R. Pittau and A. D. Polosa, JHEP **0307** (2003) 001 [arXiv:hep-ph/0206293].
- [10] R.N. Mohapatra and P.B. Pal, *Massive neutrinos in physics and astrophysics: second edition* World Sci. Lect. Notes Phys. **72** (2004) 1

- [11] G.C. Branco, L. Lavoura and J.P. Silva, *CP Violation*, Oxford University Press, Oxford, UK (1999)
- [12] J. Gluza and M. Zralek, Phys. Rev. D **55** (1997) 7030 [arXiv:hep-ph/9612227].
- [13] A. Pilaftsis, Z. Phys. C **55** (1992) 275 [arXiv:hep-ph/9901206].
- [14] F. del Aguila and J. A. Aguilar-Saavedra, JHEP **0505** (2005) 026 [arXiv:hep-ph/0503026].
- [15] S. Bergmann and A. Kagan, Nucl. Phys. B **538** (1999) 368 [arXiv:hep-ph/9803305].
- [16] B. Bekman, J. Gluza, J. Holeczek, J. Syska and M. Zralek, Phys. Rev. D **66** (2002) 093004 [arXiv:hep-ph/0207015].
- [17] C. Aalseth *et al.*, arXiv:hep-ph/0412300.
- [18] P. Benes, A. Faessler, F. Simkovic and S. Kovalenko, Phys. Rev. D **71** (2005) 077901 [arXiv:hep-ph/0501295].
- [19] G. Ingelman and J. Rathsmann, Z. Phys. C **60** (1993) 243.
- [20] D. Tommasini, G. Barenboim, J. Bernabeu and C. Jarlskog, Nucl. Phys. B **444** (1995) 451 [arXiv:hep-ph/9503228].
- [21] F. del Aguila, J. A. Aguilar-Saavedra, A. Martinez de la Ossa and D. Meloni, Phys. Lett. B **613** (2005) 170 [arXiv:hep-ph/0502189].
- [22] E. Murayama, I. Watanabe and K. Hagiwara, *HELAS: HELicity Amplitude Subroutines for Feynman Diagram Evaluations*, KEK report 91-11, January 1992.
- [23] H. K. Dreiner, P. Richardson and M. H. Seymour, Phys. Rev. D **63** (2001) 055008 [arXiv:hep-ph/0007228].
- [24] A. Abulencia *et al.* [CDF Collaboration], arXiv:hep-ex/0702051.
- [25] T. Sjostrand, S. Mrenna and P. Skands, *PYTHIA 6.4 physics and manual*, JHEP **0605** (2006) 026 [hep-ph/0603175].
- [26] M. L. Mangano, talk at Lund University,
<http://cern.ch/~mlm/talks/lund-alpgen.pdf>
- [27] E. Richter-Was, D. Froidevaux and L. Poggioli, *ATLFAST 2.0 a fast simulation package for ATLAS*, ATLAS note ATL-PHYS-98-131.

- [28] D0 Collaboration, note 5126-CONF
- [29] O. Adriani *et al.* [L3 Collaboration], Phys. Lett. B **295** (1992) 371.
- [30] P. Achard *et al.* [L3 Collaboration], Phys. Lett. B **517** (2001) 67 [arXiv:hep-ex/0107014].
- [31] S. Bray, J. S. Lee and A. Pilaftsis, arXiv:hep-ph/0702294.
- [32] G. J. Feldman and R. D. Cousins, Phys. Rev. D **57** (1998) 3873 [arXiv:physics/9711021].
- [33] G. Azuelos and A. Djouadi, Z. Phys. C **63** (1994) 327 [arXiv:hep-ph/9308340].
- [34] F. del Aguila, L. Ametller, G. L. Kane and J. Vidal, Nucl. Phys. B **334** (1990) 1.
- [35] J. A. Aguilar-Saavedra, JHEP **0612** (2006) 033 [arXiv:hep-ph/0603200].
- [36] W. Porod, M. Hirsch, J. Romao and J. W. F. Valle, Phys. Rev. D **63** (2001) 115004 [arXiv:hep-ph/0011248].
- [37] M. Hirsch and W. Porod, Phys. Rev. D **68** (2003) 115007 [arXiv:hep-ph/0307364].